MIC Overlay Coupler Design Using Spectral Domain Techniques

DONALD D. PAOLINO, MEMBER, IEEE

Abstract—A quasi-TEM analysis of dielectric overlay microstrip is described for an overlay extending several conductor linewidths beyond the coupled lines. This method permits the analysis of numerous variations of overlay coupler geometries. The relevant spectral domain Green's function is given and used to generate a set of design curves when the overlay is identical in thickness and dielectric constant to the main substrate. A trial 8.34-dB coupler was built. Significant improvement in isolation was noted with the overlay when compared to the equivalently designed uncompensated coupler. The measured values of isolation agree very well with predicted values.

I. INTRODUCTION

D IELECTRIC overlays have been used to improve isolation in microstrip directional couplers. Several quantitative analyses have been published.

Farrar and Adams [1] considered infinitely wide layered microstrip and published data for single conductor overlay microstrip. Spielman [2] used a numerical method to perform a quasi-TEM analysis for a specific overlay geometry and published computer program MICDOC [3]. Yamashita [4] used a variational method in the spectral domain for single microstrip. Krage and Haddad describe a variational analysis of numerous layered microstrip configurations [5] and treat frequency dependent overlay microstrip [6].

In this paper, the spectral domain method [7] will be used to derive a Green's function to study properties of coupled overlay microstrip.

The geometry considered is shown in Fig. 1. It is quite general in that upper ground plane, finite strip thickness, and unequal linewidths and gap spacings can be accommodated. Each region may have an arbitrary permittivity. Multiconductor capability has been incorporated into the analysis so that Lange interdigitated hybrids [8], [9] may be evaluated. Dielectric overlays for interdigitated couplers must be placed in sections with clearance gaps provided for wire bonds. Although such devices are tedious to construct, some limited experimental data are available [10]. Computation time to determine coupling characteristics is rapid in comparison with existing programs.

Materials are considered infinite in the *x* direction for application of Fourier transforms. This poses no practical restriction where a finite width overlay must be used, since the fields decay exponentially away from the conductors. Thus an overlay extending several conductor
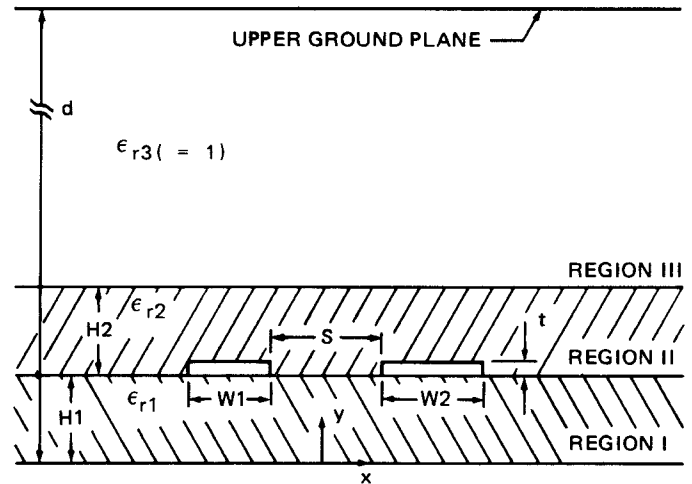
Fig. 1. Cross-sectional overlay coupler geometry.

linewidths on either side of the coupled lines is an excellent approximation to the infinite structure. Therefore, tolerance machining and placement in the *x* direction become less critical, representing a fabrication advantage.

II. THEORY

Following the spectral domain approach [7], the solution for the transform domain potential is expressed as a sum of exponentials with unknown constants in each region of Fig. 1. After applying the usual boundary conditions in the transform space, the transformed potential $\phi(\gamma, H1)$, and the transformed strip surface charge density $\rho(\gamma, H1)$ are related by

$$\phi(\gamma, H1) = G(\gamma, H1)\rho(\gamma, H1). \tag{1}$$

$G(\gamma, H1)$ is the spectral domain Green's function and is given by

$$\cfrac{1}{\epsilon_0 \gamma \left[\epsilon_{r2}\left(\cfrac{\epsilon_{r3} - \epsilon_{r2} \tanh(\gamma H2) \tanh(\gamma Q)}{\epsilon_{r3} \tanh(\gamma H2) - \epsilon_{r2} \tanh(\gamma Q)} \right) + \epsilon_{r1} \coth(\gamma H1) \right]} \tag{2}$$

where $Q = H1 + H2 - d$ and ϵ_{r1}, ϵ_{r2}, ϵ_{r3} are relative permittivities of each region. ϵ_0 is the permittivity of free space.

In the limit as $H2$ tends to 0 which describes microstrip with no overlay, (2) becomes

$$\cfrac{1}{\epsilon_0 \gamma \left[\epsilon_{r3} \coth(\gamma h2) + \epsilon_{r1} \coth(\gamma H1) \right]} \tag{3}$$

where $h2 = d - H1$. Equation (3) is exactly (10) of [7] and is the spectral domain Green's function for conventional microstrip.

Let there be N, an even number of strips with M substrips of width δx per strip. Using pulse testing functions as a basis for expanding the unknown transformed strip surface charge density, a matrix equation is obtained:

$$\sum_{n=1}^{NM} [K_{mn}][c_m] = [V_m]; \quad m = 1, NM \quad (4)$$

where K_{mn} is given by

$$\frac{4}{\pi\delta x} \int_0^\infty \cos\left(\gamma(x_n - x_m)\right)\frac{\sin^2(\gamma\delta x/2)}{\gamma^2} G(\gamma, H1)T(\gamma)\, d\gamma \quad (5)$$

and

$$T(\gamma) = 0.5(1 + \exp(-\gamma t)) \quad [4].$$

x_m and x_n are the respective field and source point coordinates which were chosen at the center of the substrip under consideration. V_m is the voltage of substrip m. This vector contains all ones for the even mode excitation.

For the odd mode:

$$V_m = +1; 1 \leqslant m \leqslant M, \quad \text{for } N = 2;$$

$$V_m = +1; (pM + 1) \leqslant m \leqslant (p+1)M,$$

$$p = 0,2,4,\cdots,N/2, \text{ for all even } N \geqslant 4;$$

$$V_m = -1; (pM + 1) \leqslant m \leqslant (p+1)M,$$

$$p = 1,3,5,\cdots,(N-1), \text{ for all even } N.$$

The c_m are solved by matrix inversion after which the static capacitance and coupling parameters of the overlay microstrip may be determined. Note that $K_{nm} = K_{mn}$ so that the entire matrix need not be stored fully in the computer.

Integration of (5) may be easily done by Simpson's rule, but is the most time-consuming part of the analysis. The integrand of (5) is well defined in the limit as γ goes to zero. It may be shown that by a simple application of l'Hospital's rule to (2) that this limit is

$$\frac{4}{\pi\delta x}\left[\frac{H1(\epsilon_{r3}H2 - \epsilon_{r2}Q)}{\epsilon_0(\epsilon_{r1}(\epsilon_{r3}H2 - \epsilon_{r2}Q) + \epsilon_{r2}\epsilon_{r3}H1)}\right]. \quad (6)$$

This term is the dominant contribution to the integral in (5). There are then no singular points within the range of integration. This is in contrast to spatial domain moment methods which have been shown to always exhibit logarithmic singularities which require special treatment [11].

The integrand in (5) decays as $1/\gamma^3$ so that the upper limit of the integral need be chosen only large enough such that the integrand is negligibly small.

Although the spectral domain approach has been shown to exhibit no singularities using pulse expansion functions, it must be remarked that Galerkin's method in the spectral domain introduces some computational diffi-
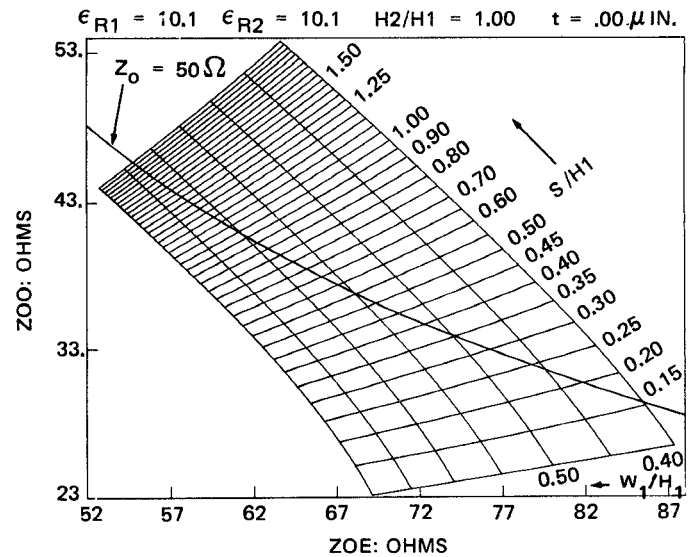

Fig. 2. Design curves ($d/H1 = \infty$).

culty in (5) because of the oscillating integrand terms. Quite a few integration points are needed for accuracy. It was initially found that results for narrow strips were quite accurate but, as the strips became wider for the same substrate thickness, accuracy decreased. This problem was traced to the oscillating integrand terms and was solved by choosing a $W/H1$ dependent scale factor for the integration variable γ. This forces the integrand numerical value to be in the same range occurring in the small $W/H1$ (≈ 0.1) case.

III. RESULTS

Using the Green's function (2) with ten substrips per strip and $W1 = W2$, a set of computer generated design curves was made for alumina overlay couplers and shown in Fig. 2. Typical computation time on the Univac 1110 computer was 23 s per grid point. The results of the program were compared against those of Bryant and Weiss. Typical convergence trials for the coupling coefficient using ten substrips per strip agreed to within 2 percent.

Fig. 3 shows the results of a 50-Ω 8.34-dB overlay coupler designed from Fig. 2. Note that approximately 10-dB isolation improvement is obtained over the equivalently designed uncompensated coupler. The ABCD matrix method of Levy [12] was employed to calculate theoretical isolation values. The coupler was designed for a 2-GHz center frequency so that connector and transition effects would minimally affect the measurements. The theoretical and actual measured isolation values agree quite well.

The overlay improves coupler isolation by increasing the effective odd mode dielectric constant while correspondingly decreasing the even mode effective dielectric constant. The ratio of odd mode phase velocity v_o to even mode phase velocity, v_e, for the uncompensated 8.34-dB coupler was 1.115 while the overlay device $v_o/v_e = 0.940$. Thus compared with the nonoverlay coupler, a mode
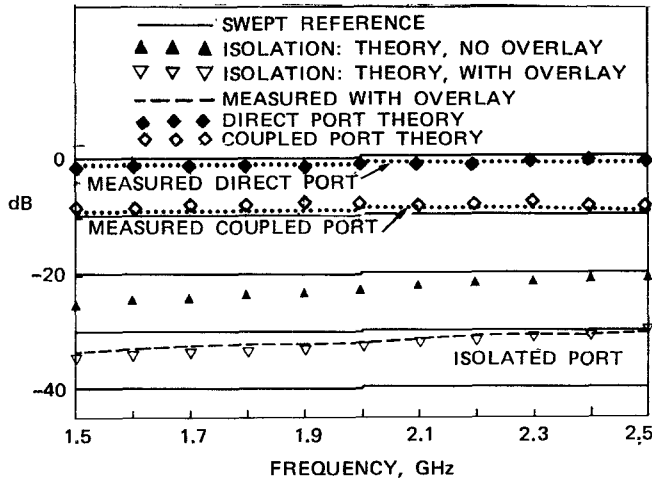
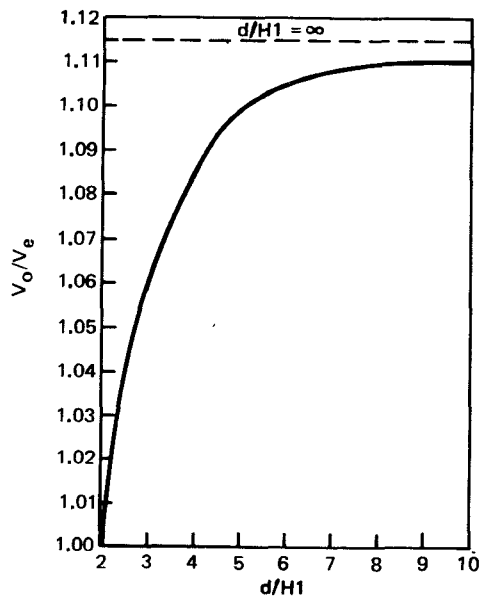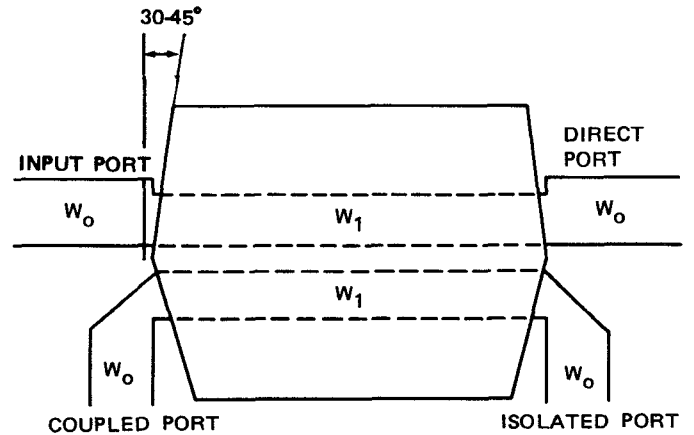Fig. 3.   Comparison of theoretical and measured coupler insertion loss.

Fig. 5.   Plan view of dielectric overlay coupler and bevel detail.

optimum design consistent with physically realizable line-widths and gap spacings.

IV. FABRICATION DETAILS

It is of utmost importance that air gaps be eliminated during overlay placement. The technique used was to soften the overlay with a suitable solvent. The overlay is placed over the coupled lines and causes the material to conform to the conductor contours. The overlay is clamped in place after which an adhesive may be used on the overlay edges to ensure firm placement. Results reported here were obtained with Custom Materials Incorporated type Hi K 707L-10 overlay material which softens easily using acetone as a solvent.

It is also critical that the overlay edges not come in contact with the connecting lines to the coupled conductors because of the charge density singularity at the strip edges.

With a network analyzer set up to measure isolation, a rectangular shaped overlay in a softened condition was placed over the coupling gap. Significant deviation from theoretical isolation values was observed as the overlay edges only slightly contacted the port connecting lines. To avoid costly tolerance overlay grinding or alignment sensitivity, a beveled edge overlay form shown in Fig. 5 was found to alleviate these two problems for this geometry.

One advantage of the Sheleg and Spielman type overlay [2] is that proximity effects on input–output lines are reduced since the overlay width is designed to just span the distance across the coupled conductors. However, cement of the same relative permittivity as the overlay and substrate was applied to the overlay underside where the fields are fairly strong. Any trapped air bubbles or other adhesive inhomogeneities would have a greater effect on coupler isolation than in a wide beveled edge overlay, since the bonding agent (which may have arbitrary permittivity) is applied only to overlay outer edges where field amplitudes are comparatively weak.

Fig. 4.   Ratio of even to odd mode phase velocities versus $d/H1$ for Fig. 1 configuration ($\epsilon_{r1}=10.1$, $\epsilon_{r2}=10.1$, $W1/H1=0.740$, $S/H1=0.175$).

velocity ratio closer to the theoretically infinite isolation condition ($v_o/v_e=1.00$) is achieved.

Mode velocity equalization can be accomplished without using dielectric overlays by placing the upper ground plane in close proximity to the coupled strips [5], [13]. Equations (2), (4), and (5) were used to investigate ground plane effects on mode velocity ratio as a function of $d/H1$ (Fig. 4). The value of $d/H1=2.0$ given in Fig. 4 corresponds to $v_o/v_e=1.00$ and thus the mode velocities are essentially equalized.

Design curves similar to Fig. 2 were made for $H2/H1=0.4$, but the isolation was typically 3 dB lower across the same frequency band than for $H2/H1=1.00$. For optimizing isolation, a series of design curves could be constructed with $H2/H1$ and $\epsilon_{r1}/\epsilon_{r2}$ as parameters. v_o/v_e could be examined for a desired coupling value, and the mode velocity ratio closest to unity would identify the

V. CONCLUSIONS

The spectral domain approach has been shown to produce design information allowing significant improvement

in MIC coupler isolation. Advantages of this method over spatial domain treatments include absence of singular integrals and efficient treatment of finite strip thickness and upper ground plane effects. The need for scaling techniques to allow analysis of a large dynamic range of strip parameters has been pointed out as a limitation. Good agreement between experimental and computed values of isolation was obtained.

Possible applications of these results could allow improved coupler design, improvement in midband VSWR of Schiffman phase shifters [14], or improved MIC filter response.

ACKNOWLEDGMENT

The author wishes to thank J. A. Mosko for valuable comments on fabrication techniques and Prof. A. T. Adams for help in the preparation of this paper.

REFERENCES

[1] A. Farrar and A. T. Adams, "Multilayer microstrip transmission lines," *IEEE Trans. Microwave Theory Tech.*, vol. MTT-22, pp. 889–891, Oct. 1974.
[2] B. Sheleg and B. E. Spielman, "Broad band directional couplers using microstrip with dielectric overlays," *IEEE Trans. Microwave Theory Tech.*, vol. MTT-22, pp. 1216–1219, Dec. 1974.
[3] B. E. Spielman, "Analysis of electrical characteristics of edge coupled microstrip lines with a dielectric overlay," NRL Report 7810, Oct. 1974.
[4] E. Yamashita and R. Mittra, "Variational method for the analysis of microstrip lines," *IEEE Trans. Microwave Theory Tech.*, vol. MTT-16, pp. 251–256, Apr. 1968.
[5] M. K. Krage and G. I. Haddad, "Characteristics of coupled microstrip transmission lines-II: Evaluation of coupled line parameters," *IEEE Trans. Microwave Theory and Tech.*, vol. MTT-18, pp. 222–228, Apr. 1970.
[6] ——, "Frequency dependent characteristics of microstrip transmission lines," *IEEE Trans. Microwave Theory and Tech.*, vol. MTT-20, pp. 678–688, Oct. 1972.
[7] Y. Rahmat-Samii *et al.*, "A spectral domain analysis for solving microstrip discontinuity problems," *IEEE Trans. Microwave Theory Tech.*, vol. MTT-22, pp. 372–378, Apr. 1974.
[8] R. Waugh and D. Lacombe, "Unfolding the Lange coupler," *IEEE Trans. Microwave Theory Tech.*, vol. MTT-20, pp. 77–79, Nov. 1972.
[9] D. D. Paolino, "Design more accurate interdigitated couplers, Microwaves," vol. 15, pp. 34–38, May 1976.
[10] C. Buntschuh, "Octave bandwidth high-directivity microstrip couplers," in *Microwave Associates*, Burlington MA, Tech Rept. RADC-TR-73-396, Jan. 1974.
[11] P. Silvester and P. Benedek, "Electrostatics of the microstrip-revisited," *IEEE Trans. Microwave Theory Tech.*, vol. MTT-20, pp. 756–758, Nov. 1972.
[12] R. Levy, in *Advances in Microwaves*, vol. 1, Ed., Leo Young. New York: Academic Press, 1966, pps. 125–128.
[13] M. H. Arain and N. W. Spencer, "Tapered microstrip magic tee," *IEEE Trans. Microwave Theory and Tech.*, vol. MTT-23, pp. 1064–1067, Dec. 1975.
[14] A. Podell, "Use these latest techniques to improve your GHz circuits," *Electronic Design News*, vol. 15, no. 1, pp. 56–59, Jan. 5, 1974.

Some Results on the End Effects of Microstriplines

CHANDRA GUPTA, STUDENT MEMBER,IEEE, BRIAN EASTER, AND ANAND GOPINATH, MEMBER, IEEE

Abstract—A new resonant technique for accurate and reliable measurement of end and gap effects in microstripline has been developed. An investigation of the frequency dependence of end and gap effects in microstrip was performed. There is no apparent frequency variation for the end effects for $w/h = 0.5$, 1.0, and 2.0 lines on alumina substrate ($\epsilon_r \approx 9.8$), between 7.0 and 18.0 GHz. A small dependence on resonator mode number of these effects has been observed.

I. INTRODUCTION

MICROSTRIP open-ends are used in variety of stripline matching and filter circuits. The characterization of small microstrip discontinuities such as cross-over requires a very accurate knowledge of end effects for the resonant structure. Therefore, open-ends constitute an important class of microstrip discontinuity. Static calculations [1]–[3] provide accurate estimates of the capacitance due to the fringe fields at the open. However, the behavior of this shunt capacitance or equivalent series line length l_o with frequency has not been examined in any detail [4]. The present paper reports on the results of an experimental investigation of the frequency dependence of the microstrip open-end capacitance or equivalent line length l_o. An accurate method of measurement which is an extension of the resonant technique has been developed in the course of this work. Furthermore, the frequency dependence of the series gap equivalent circuit line length l_g has also been examined.

The resonances of lengths of straight microstrip resona-